Basic Folded and Low-Populated Locally Disordered Conformers of SUMO-2 Characterized by NMR Spectroscopy at Varying Pressures†

Ryo Kitahara,‡ Chenhua Zhao,§ Kohei Saito,§ Seizo Koshiba,§ Makoto Ioune,§ Takanori Kigawa,§,|| Shigeyuki Yokoyama,‡,§,⊥ and Kazuyuki Akasaka*,‡,@

RIKEN SPring-8 Center, 1-1-1 Kouto, Sayo-cho, Sayo-gun, Hyogo 679-5148, Japan, RIKEN Genomic Sciences Center, 1-7-22 Suehiro-cho, Tsurumi-ku, Yokohama 230-0045, Japan, Department of Computational Intelligence and Systems Science, Interdisciplinary Graduate School of Science and Engineering, Tokyo Institute of Technology, 4259 Nagatsuta-cho, Midori-ku, Yokohama 226-8502, Japan, Department of Biophysics and Biochemistry, Graduate School of Science, The University of Tokyo, 7-3-1 Hongo, Bunkyo-ku, Tokyo 113-0033, Japan, and Department of Biotechnological Science, School of Biology-Oriented Science and Technology, Kinki University, 930 Nishimitani, Kinokawa, Wakayama 649-6493, Japan

Received July 22, 2007; Revised Manuscript Received October 28, 2007

ABSTRACT: SUMO proteins, a group of post-translational ubiquitin-like modifiers, have target enzymes (E1 and E2) like other ubiquitin-like modifiers, e.g., ubiquitin and NEDD8, but their physiological roles are quite different. In an effort to determine the characteristic molecular design of ubiquitin-like modifiers, we have investigated the structure of human SUMO-2 in solution not only in its basic folded state but also in its higher-energy state by utilizing standard and variable-pressure NMR spectroscopy, respectively. We have determined average coordinates of the basic folded conformer at ambient pressure, which gives a backbone structure almost identical with those of ubiquitin and NEDD8. We have further investigated conformational fluctuations in a wide conformational space using variable-pressure NMR spectroscopy in the range of 30−3 kbar, by which we find a low-populated (∼2.5%) alternative conformer preferentially disordered in the enzyme-binding segment. The alternative conformer is structurally very close to but markedly different in equilibrium population from those for ubiquitin and NEDD8. These results support our notion that post-translational ubiquitin-like modifiers are evolutionarily designed for function both structurally and thermodynamically in their low-populated, high-energy conformers rather than in their basic folded conformers.

Several classes of proteins having identical topology of folding with ubiquitin (*1*, *2*), called ubiquitin-like proteins (UBLs),[1] regulate metabolic stabilities of proteins and modify their functions in living cells by post-translational modification (*1*−*5*). SUMO proteins, a class of modifier UBLs, have been implicated for their roles in nuclear transport, regulation of transcription, and cell division (*1*, *4*, *6*−*9*). SUMO proteins have similar chemistry with ubiquitin and NEDD8; namely, they are attached to target proteins via formation of an isopeptide bond between its C-terminal glycine and a specific lysine side chain of the target protein. In mammals, at least four different SUMO proteins, SUMO-1, -2, -3, and -4, are found (*7*, *10*). The basic folded structure is known for only SUMO-1 (*11*) and SUMO-3 (*12*) in solution and for SUMO-2 (*13*) in crystal. The crystal structure of SUMO-2 has a topology of folding quite similar to those of ubiquitin and SUMO-1, although the level of sequence identity of SUMO-2 with ubiquitin is low (18%).

Here we determine the basic folded structure of SUMO-2 in solution with standard NMR techniques, study its rapid internal dynamics with spin relaxation, and investigate its slow conformational fluctuations in a wide conformational space using variable-pressure $^{15}N-^{1}H$ two-dimensional NMR spectroscopy. The results are compared with those found previously for ubiquitin (*14*−*16*) and NEDD8 (*17*) in characterizing the structural and thermodynamic design of SUMO-2 for function.

MATERIALS AND METHODS

Protein Sample Preparation. The gene encoding full-length human SUMO-2 was cloned into plasmid vector PCR2.1 from cDNA clone CAS08355 of the Sugano cDNA library as a fusion with an N-terminal HAT affinity tag and a TEV protease cleavage site. The uniformly ^{13}C- and ^{15}N-labeled SUMO-2 protein was produced by the *Escherichia coli* cell-free protein expression system described previously (*18*−*20*). For the NMR experiments, the uniformly ^{13}C- and

† This work was carried out under JSPS Research Fellowships for Young Scientists (R.K.), JSPS Core-to-Core Program-Integrated Action Initiative 17009, and the RIKEN Structural Genomics/Proteomics Initiative (RSGI).

* To whom correspondence should be addressed: Department of Biotechnological Science, School of Biology-Oriented Science and Technology, Kinki University, 930 Nishimitani, Kinokawa, Wakayama 649-6493, Japan. Telephone: +81-736-77-3888. Fax: +81-736-77-4754. E-mail: akasaka@waka.kindai.ac.jp.

‡ RIKEN SPring-8 Center.

§ RIKEN Genomic Sciences Center.

|| Tokyo Institute of Technology.

⊥ The University of Tokyo.

@ Kinki University.

[1] Abbreviations: N, basic folded conformer; I, alternative conformer; U, unfolded conformer; HSQC, heteronuclear single-quantum coherence; SUMO, small ubiquitin-related modifier; UBL, ubiquitin-like protein.

10.1021/bi7014458 CCC: $40.75
Published on Web 12/15/2007

^{15}N-labeled SUMO-2 protein was concentrated to 1.2 mM in 20 mM [^{2}H]Tris-HCl buffer (pH 7.0) containing 100 mM NaCl, 1 mM [^{2}H]DTT, 0.02% NaN_3, and a 10% $^{2}H_2O$/90% $^{1}H_2O$ mixture (v/v). The protein used for the NMR measurements consists of 104 amino acid residues, including tag sequences at the N-terminus (GSSGSSG) and at the C-terminus (SGPSSG) used for expression and purification. In this paper, the amino acid numbering is chosen to be consistent with that of the native amino acid sequence.

Determination of the NMR Structure at Atmospheric Pressure. All the NMR spectra were recorded in a SIGEMI tube with an outer diameter of 5 mm at 25 °C on an AVANCE 600 or 800 spectrometer (Bruker Biospin Co.) equipped with a full-field gradient triple-resonance probe. Sequence-specific resonance assignments were achieved using the standard triple-resonance techniques (*21*−*24*). Standard two-dimensional (2D) ^{15}N−^{1}H HSQC, three-dimensional (3D) HNCO, HN(CA)CO, HNCA, HN(CO)CA, CBCA(CO)NH, and HNCACB pulse sequences were employed for the protein backbone assignments. 2D ^{13}C−^{1}H HSQC, 3D HBHA(CO)NH, CCCONNH, HCCCONNH, HCCH-TOCSY, and HCCH-COSY data were collected for the assignments of the aliphatic side chain CH_n, including all prolines. The aromatic ring resonances were identified by the HCCH-COSY and ^{13}C-edited ^{1}H−^{1}H NOESY-HSQC experiments in the aromatic region. All the assignments were checked for the consistency with 3D ^{15}N-edited ^{1}H−^{1}H NOESY-HSQC and ^{13}C-edited ^{1}H−^{1}H NOESY-HSQC spectra (mixing time of 80 ms). All the NMR spectra were processed with NMRPipe (*25*) and visualized and analyzed with NMRview (*26*) with the help of KUJIRA (*27*).

The distance constraints for the structural calculation were generated from the 3D ^{15}N-edited ^{1}H−^{1}H NOESY-HSQC and ^{13}C-edited ^{1}H−^{1}H NOESY-HSQC spectra obtained with a mixing time of 80 ms. All five Pro residues in SUMO-2 are in the *trans* conformation, as revealed by chemical shift differences in C_β and C_γ (*28*) and by relative NOE strengths between $H_\alpha(i)$−$H_\alpha(i-1)$ and $H_\delta(i)$−$H_\alpha(i-1)$ (*3*). Stereospecific signal assignments were made for Val and Leu methyl groups when their two methyl groups were distinguished from their difference in the ^{13}C-edited NOESY-HSQC pattern. For the stereochemically ambiguous protons, pseudoatom correction was added to the upper bounds for both methylene and chemically equivalent aromatic protons. Backbone dihedral restraints (φ and ψ) were derived from the prediction program named TALOS (*29*). The 3D protein structure was determined by the automated NOE cross-peak assignments program CANDID, followed by structure calculation with torsion angle dynamics (*30*) using CYANA (version 2.0.17). Twenty conformers with the lowest target function in cycle 7 of CYANA were chosen, and PROCHECK (*31*) and MOMOL (*32*) were used to validate and to visualize the final structures, respectively. The statistics of the structures, including the distance and torsion angle constraints used for the structure calculation, are summarized in Table 1. More than 97% of the automatically picked NOE cross-peaks were assigned, and a total of 1626 NOE distance restraints and 86 dihedral angle restraints (43 φ and 43 ψ) were used in CYANA refinement calculations (*33*), giving CYANA target functions of 0.04 ± 0.01 Å^2. The average root-mean-square deviation (rmsd) from the mean structure for the backbone of the ordered residues was 0.22 Å. None of these structures have distance violations of >0.1 Å or dihedral angle violations of >2°. The Ramachandran plot of the ϕ and ψ angles (from Asn14 to Thr91) for the 20 structures shows 85.6% of the ϕ and ψ angles to be in the most favored regions, 14.1% in the additionally allowed regions, 0.4% in the generously allowed regions, and 0% in the disallowed regions. These statistics show that these structural models are fully consistent with the experimentally obtained restraints. The 20 models are deposited in the Protein Data Bank (entry 1WZ0).

Table 1: Statistics for the Final Ensemble (20 structures)[a]

no. of distance restraints	1626
intraresidue and sequential ($\|i-j\| \leq 1$)	810
medium-range ($1 < \|i-j\| < 5$)	252
long-range ($\|i-j\| \geq 5$)	564
no. of torsion angle restraints	86
CYANA target function value	0.038 ± 0.013
no. of distance restraint violations	
number >0.1 Å	0
maximum	0
no. of torsion angle restraint violations	
number >5°	0
maximum	0
rms deviation from the mean structure	
backbone atoms (residues 14−91)	0.708 Å
all heavy atoms (residues 14−91)	1.217 Å
backbone regions (ordered region)	0.223 Å
all heavy atoms (ordered region)	0.648 Å
Ramachandran plot analysis (residues 14−91)[b]	
residues in favored regions	85.6%
residues in additionally allowed regions	14.1%
residues in generously allowed regions	0.4%
residues in disallowed regions	0.0%

[a] The protein sample used for the NMR measurements consists of 104 amino acid residues, including tag sequences at the N-terminus (GSSGSSG) and at the C-terminus (SGPSSG) used for expression and purification, respectively. In this paper, the amino acid numbering consistent with that of the original SUMO-2 sequence is employed. In the PDB table, the numbering includes the tag sequences in the N- and C-termini. [b] Determined with PROCHECK-NMR.

Variable-Pressure NMR Experiments. Variable-pressure NMR experiments were performed in a homemade pressure-resistive quartz cell with an outer diameter of ∼3.5 mm and an inner diameter of ∼1 mm in the pressure range between 30 and 3000 bar on a DRX 800 spectrometer (Bruker Biospin Co.) using the on-line cell variable-pressure NMR method (*34*, *35*). The design details of the pressure-resistive NMR cell are described elsewhere (*36*).

The proton NMR spectra were measured at a proton frequency of 800.16 MHz using a 3-9-19 pulsed field gradient for water suppression. ^{15}N−^{1}H HSQC spectra were recorded with a sensitivity enhancement HSQC sequence at a proton frequency of 800.16 MHz and a ^{15}N frequency of 81.08 MHz. Two hundred increments were used for the t_1 (^{15}N) dimension, and 2048 complex points were collected for the t_2 (proton) dimension with an offset at the residual water signal. The relaxation delay was set to 1.5 s for each

scan. At all pressures, ^{1}H chemical shifts were referenced to the methyl signal of 2,2-dimethyl-2-silapentane-5-sulfonate (DSS), and ^{15}N chemical shifts were indirectly referenced to DSS (0 ppm for ^{1}H). The data points were extended to 2K × 512 with linear prediction, and 90°-shifted sine-bell window functions were applied in both dimensions. Data were processed with XWIN-NMR (Bruker Biospin Co.), NMRPipe (*25*), and NMRview (*26*).

Thermodynamic Analysis. Under physiological conditions at 1 bar, the protein is nearly fully folded in conformer N, giving NMR signal intensity I_{0i} for site *i*. With an increase in pressure, either a local or an overall unfolding takes place into another conformer, U, and then the original signal intensity (I_{0i}) for site *i* decreases to I_i. The decrease in the intensity ($I_0 - I_i$) divided by the intensity I_i represents the equilibrium constant $([U]/[N])_i$ at site *i*. Namely

$$K_i = ([U]/[N])_i = (I_0 - I_i)/I_i \quad (1)$$

In actual applications, I_i may represent individual cross-peak intensities in two-dimensional HSQC spectra or the integral intensity of a well-separated signal in the one-dimensional ^{1}H NMR spectra.

On the other hand, the Gibbs energy difference ΔG between the two conformers is expressed as a function of pressure *p* by eq 2 under the assumption of negligible changes of differential compressibility with pressure between the two conformers:

$$\Delta G^p = -RT \ln K = \Delta G^0 + \Delta V^0(p - p_0) \quad (2)$$

where *R* is the gas constant, *T* is the absolute temperature, *K* is the equilibrium constant, and ΔG^p and ΔG^0 are the Gibbs free energy differences at pressure *p* and p_0 (=1 bar), respectively. ΔV^0 is the partial molar volume difference between the two conformers extrapolated to pressure p_0 (=1 bar).

RESULTS AND DISCUSSION

Structure of the Basic Folded Conformer in Solution. The sequence of SUMO-2 is 18% identical with that of ubiquitin. The sequence alignment of ubiquitin and NEDD8 is shown in Figure 1A. The structure of the basic folded conformer of SUMO-2 was determined at ambient pressure using standard NMR techniques as described in Materials and Methods. Table 1 lists the statistics for the final 20 structures calculated by CYANA. The rms deviation from the mean structure is 0.22 Å for the backbone atoms.

Figure 1B shows the final 20 structures of SUMO-2, shown as a backbone superposition of the 20 low-energy conformers from the CYANA calculation (*33*) (left, the N-terminal segment, residues 1−13; middle and right, residues from position 14 to the C-terminus viewed from two different angles). The solution structure of SUMO-2 has the $\beta\beta\alpha\beta\beta\alpha\beta$ ubiquitin fold (Figure 1B, middle and right), with an additional long flexible N-terminal segment (Figure 1B, left) which is not present in ubiquitin and NEDD8. The function of the long N-terminus is not known. Figure 2 summarizes NOE patterns for the polypeptide backbone of SUMO-2. Interestingly, several middle-range NOEs are observed within the flexible N-terminal segments (residues 3−7), giving a weakly ordered conformation with hinges at residues 13−18.

Figure 1C shows a comparison of the solution structure (blue) and the crystal structure (*13*) (red). The overall three-dimensional structure, the hydrogen bonding network, and the molecular surface are closely identical between the two structures for the core part (residues 17−87) with a rmsd of 1.09 Å for the backbone atoms. The only clear difference between the crystal and solution structures is in the side chain orientation of Leu43 located in the hydrophobic core part; a χ_2 of 60° is preferred in solution, while a χ_2 of 180° is preferred in crystal. Finally, Figure 1D gives a superposition of the solution structures of SUMO-1 (*11*), SUMO-2 (this work), and SUMO-3 (*12*). The rmsd of the backbone is 2.05 Å between SUMO-2 and SUMO-3 (sequence identity of 87%) and 3.47 Å between SUMO-2 and SUMO-1 (sequence identity of 47%). Clearly, the backbone folds are closely similar to each other among the three proteins.

Picosecond-to-Nanosecond Dynamics of the Basic Folded Conformer at High and Low Pressure. To characterize the picosecond-to-nanosecond dynamics of SUMO-2 in solution, we measured ^{15}N spin relaxation parameters R_1, R_2, and heteronuclear NOE in the laboratory frame for individual amide nitrogens of the backbone at 30 bar and 1 kbar at 25 °C (Figure 3). At 30 bar, the R_1 (Figure 3A) and NOE (Figure 3C) values showed little variation among residues 18−87 (the folded part) except for residues 54−57 in a turn region, while heteronuclear NOE decreased for residues below position 18 and beyond position 87. The results indicate fairly uniform internal motions in the picosecond-to-nanosecond time range for residues 18−87, which increase progressively toward the N- and C-terminal ends. The average R_1 and NOE values for residues in the folded part are nearly identical between SUMO-2 and ubiquitin (*16*), showing that the fast dynamics of the backbone in this time range is similar for the two proteins. The R_2 value also exhibited little variation among residues 18−87 (Figure 3B), as in the case of ubiquitin at 1 bar. The fact that the R_2 value averaged for residues 18−87 (12.9 s^{-1}) is slightly larger than that for ubiquitin (9 s^{-1}) (*16*) can be attributed to the difference in molecular mass between the two proteins (SUMO-2, 12.5 kDa; ubiquitin, 8.6 kDa).

The three relaxation parameters R_1, R_2, and NOE did not exhibit appreciable changes between 30 bar and 1 kbar, except for a small change in R_1 in the N-terminal segment (Figure 3A). The result indicates that the fast (picosecond-to-nanosecond) dynamics of the polypeptide chain of SUMO-2 is not sensitive to pressure at least up to 1 kbar. Relaxation measurements could not be extended beyond 1 kbar for SUMO-2, because of the substantial decrease in signal intensity for many cross-peaks.

Fluctuations within the Folded Ensemble from Pressure-Induced Chemical Shifts. Variable-pressure NMR spectroscopy allows one to study conformational fluctuations of a protein in a much wider conformational space and a much wider time range than most other techniques can (*34*). Variable-pressure ^{1}H one-dimensional and ^{15}N−^{1}H two-dimensional HSQC measurements were performed on uniformly ^{13}C- and ^{15}N-labeled SUMO-2 at 25 °C between 30 bar and 3 kbar. Figure 4 shows a superposition of the ^{15}N−^{1}H HSQC spectra obtained at various pressures between 30 bar and 3 kbar. We note chemical shift changes continuously

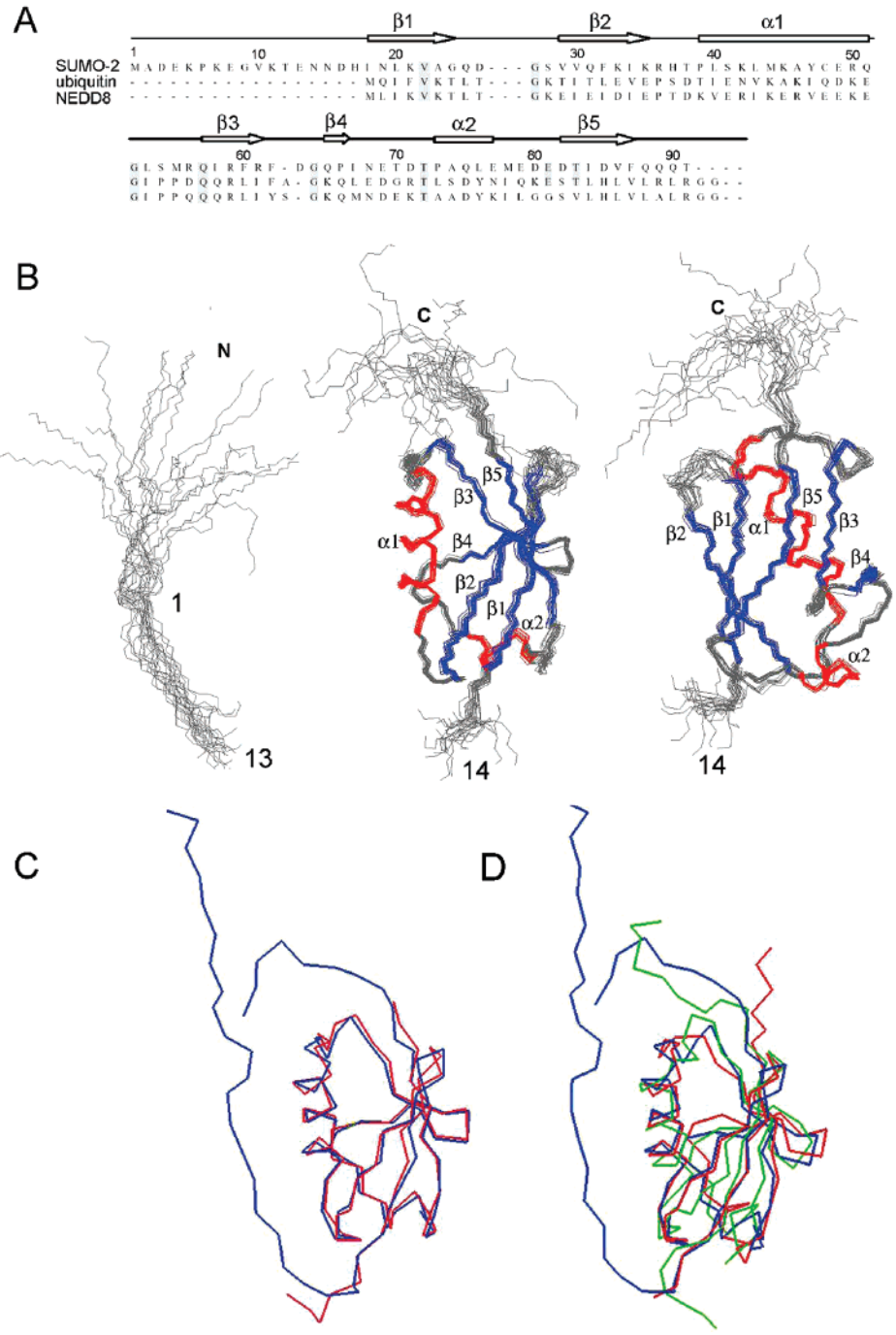

FIGURE 1: (A) Structure-based sequence alignment of SUMO-2, ubiquitin, and NEDD8 from humans. (B) NMR structures of human SUMO-2 (pH 7.0 and 25 °C), shown as a backbone superposition of 20 lower-energy conformers from the CYANA calculation (*33*) (left, N-terminus to residue 13; middle and right, two different views for residues from position 14 to the C-terminus). (C) Comparison between the solution structure [blue (this work)] and the crystal structure [red (*13*)] of SUMO-2. (D) Comparison between the solution structures of SUMO-1 [green (*11*)], SUMO-2 [blue (this work)], and SUMO-3 [red (*13*)].

with pressure for practically all the cross-peaks in the spectra. In addition, substantial reduction of signal intensities takes place for some cross-peaks with an increase in pressure. All the spectral changes are reversible with pressure.

Figure 5 visualizes changes in pressure-induced ^{15}N (panel A) and ^{1}H (panel B) chemical shifts at 1 kbar for individual residues. The average changes in ^{15}N and ^{1}H shifts at 1 kbar are 0.26 ± 0.21 and 0.031 ± 0.041 (average ± rmsd), respectively. The average pressure-induced shifts for ^{15}N and ^{1}H of SUMO-2 are comparable with those of ubiquitin (0.19 ppm for ^{15}N and 0.03 ppm for ^{1}H). The unusual chemical shift changes, either positive or negative, are observed for several residues, especially residues 38, 40, 41, 43, 58, and 70 in ^{15}N and residues 24, 38, 41, 43, 46, 52, 65, and 70 in ^{1}H. Many residues are located between residues 38 and 46, namely, the N-terminal half of the α_1 helix and just before the helix. The residue-specific chemical shift response to a small variation of pressure within a range of a few kilobars is a direct manifestation of equilibrium fluctuations of the protein occurring in the time range of much less than milliseconds at ambient pressure (*34*, *35*). Thus, the result of Figure 5 indicates that the protein structure fluctuates

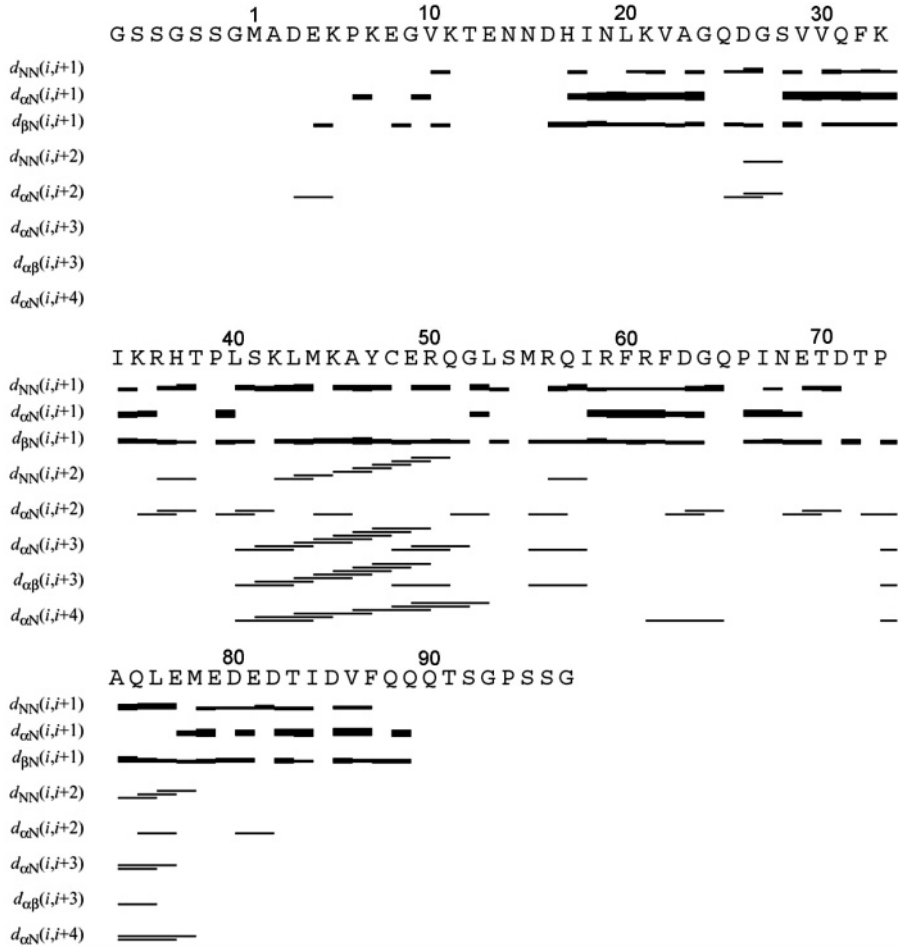

FIGURE 2: Summary of sequential and medium-range NOE patterns observed in SUMO-2. The data were derived from ^{15}N-edited and ^{13}C-edited NOESY-HSQC experiments (mixing time of 80 ms) performed on a 1.2 mM solution of uniformly ^{13}C- and ^{15}N-labeled SUMO-2 at pH 7.0 and 25 °C.

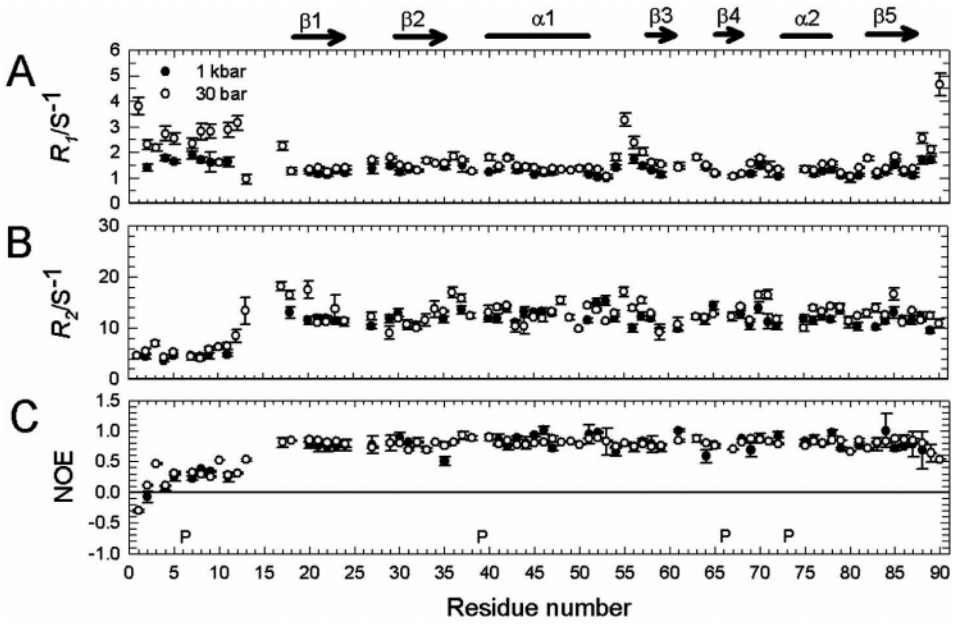

FIGURE 3: Spin relaxation dynamics of SUMO-2 at 30 bar (○) and at 1 kbar (●). (A) ^{15}N longitudinal relaxation rates (^{15}N-R_1). (B) ^{15}N transverse relaxation rates (^{15}N-R_2). (C) ^{1}H-induced ^{15}N nuclear Overhauser effects (^{15}N{^{1}H} NOE). P designates proline residues (P6, P39, P66, and P73) having no amide groups.

heterogeneously within the native state ensemble, probably with a hinge-type motion at the N-terminal half of the α_1 helix and just before the helix.

Conformational fluctuations of SUMO-1, a protein related to SUMO-2 (sequence identity of 47%), in the native state ensemble have also been reported by Kumar et al. (*37*) on

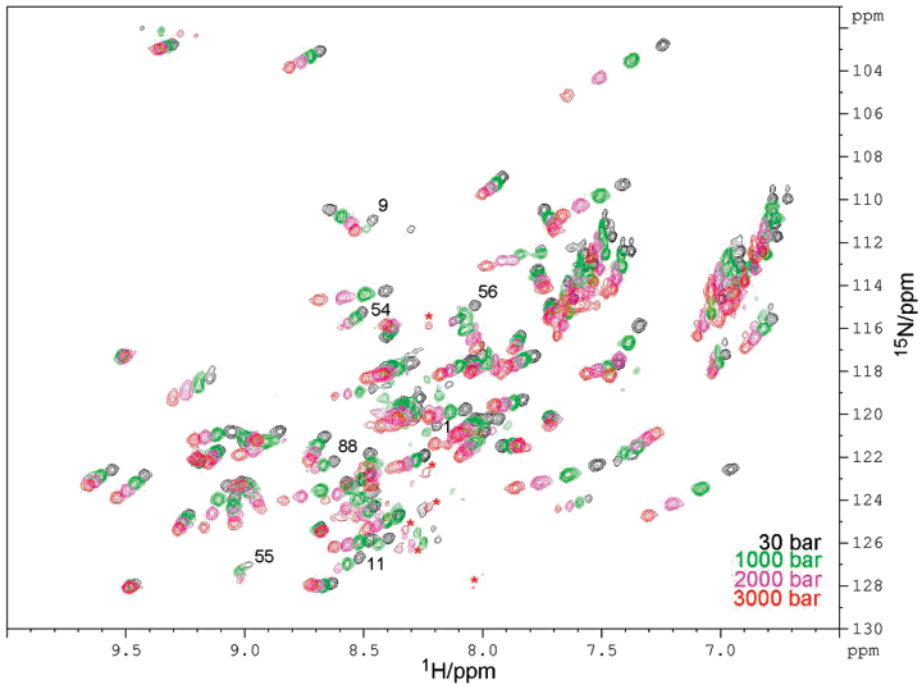

FIGURE 4: Overlaid plot of the ^{15}N−^{1}H HSQC spectra of SUMO-2 as a function of pressure. The experiments were performed on 1.2 mM uniformly ^{13}C- and ^{15}N-labeled SUMO-2 at 25 °C in 20 mM [^{2}H]Tris-HCl buffer (pH 7.0) containing 100 mM NaCl, 1 mM [^{2}H]DTT, 0.02% NaN_3, and a 10% $^{2}H_2O$/90% $^{1}H_2O$ mixture (v/v).

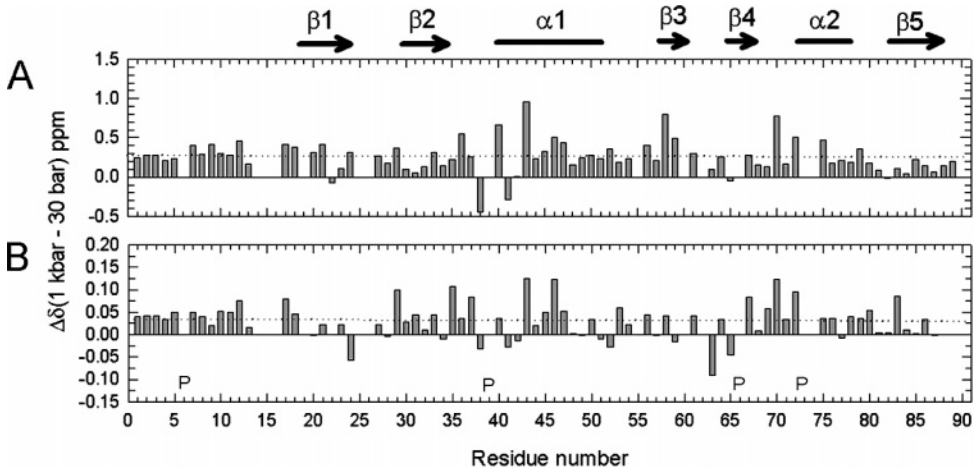

FIGURE 5: Pressure-induced chemical shifts ($\Delta\delta = \delta_{1kbar} - \delta_{30bar}$) of amide ^{15}N (A) and ^{1}H (B) plotted against the amino acid sequence of SUMO-2. The average values of ^{15}N (0.26 ± 0.21) and ^{1}H (0.031 ± 0.041) pressure shifts are shown by dotted lines. Proline residues are indicated by P in the bottom panel.

the basis of the nonlinear dependence of amide proton chemical shifts on temperature in the presence of subdenaturing concentrations of urea (0−0.9 M). This analysis is based on the assumption that a small concentration of urea amplifies but does not alter the intrinsic fluctuation of the protein in its native ensemble. Peculiar nonlinear chemical shifts against the variation in temperature are found at several regions of the protein, some of which coincide with the binding surfaces of the target proteins, including E1, E2, and SUMO binding motifs (*37*, *38*). Since the method shares some common ground with chemical shift perturbations by pressure, comparison of the two results is expected to give further insight into conformational fluctuations in SUMO family proteins within the native state ensemble. We defer, however, such a comparison in later occasions, as our pressure shift data are currently limited within a narrow pressure range (<1 kbar).

Structure of the Low-Populated Locally Disordered Conformer. Figure 6 plots cross-peak intensities (volumes) in the ^{15}N−^{1}H HSQC spectra against pressure (Figure 4) for individual residues of SUMO-2, each normalized to the intensity at 30 bar. Cross-peak intensities are found preferentially reduced with increasing pressure, reaching nearly null at 3 kbar, for residues 1, 2, 7−9, 11, 17, 54−56, and 88−90 (Figure 6A). These residues are located in the aligned N-terminal segments and in the proximity of the C-terminal side of the protein (cf. Figure 7A).

Among these, the cross-peak intensity changes for the N-terminal segments [residues 1−17 (Figure 6A)] are distinctly noncooperative, suggesting a heterogeneous disorder of the weakly structured N-terminal segments. On the other hand, the nearly simultaneous changes of the cross-peak intensities for the residues in the proximity of the C-terminus (residues 54, 56, 88, and 89), except for residues

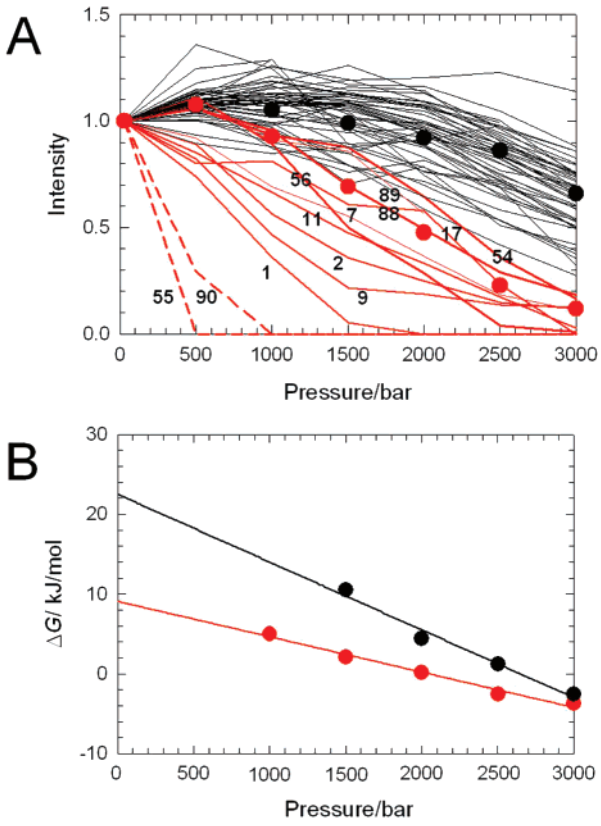

FIGURE 6: (A) Plots of intensities (volumes normalized at 30 bar) of all observable cross-peaks in the $^{15}N-^{1}H$ HSQC spectra of SUMO-2 at different pressures (30, 500, 1000, 1500, 2000, 2500, and 3000 bar) at pH 7.0 and 25 °C. Intensity corrections are made for the pressure-induced compaction of the solvent water (e.g., by ~9% at 3 kbar). The cross-peaks can be classified into two groups: the rapidly decaying group (red, residues 1, 2, 7−9, 11, 17, 54−56, and 88−90; with exceptionally rapid decaying residues being red circles) and the slowly decaying group (black, the rest). Nearly cooperative transition curves observed for the residues in the proximity of the C-terminus (5−56 and 88−90) and those for the slowly decaying group are averaged (marked by red filled circles and black filled circles, respectively). (B) Plots of stability difference, ΔG_{NI} and ΔG_{NU}, against pressure (see eqs 1 and 2 for evaluation of ΔG_{NI} and ΔG_{NU} values). The thermodynamic parameters, ΔG^0 and ΔV^0, are obtained by a least-squares fit of K to eq 2 under the assumption of zero compressibility difference (*15*). Extrapolation to 1 bar yields the ΔG^0. The slopes give ΔV^0 for the transitions.

55 and 90, suggest that the part in the proximity of the C-terminus undergoes a fairly cooperative transition, the average of the intensities represented by filled circles with a half-transition at ~1500 bar in Figure 6A. Only a few cross-peaks appear newly in the region for a typical unfolded polypeptide chain (8.0−8.6 ppm for peptide ^{1}HN signals) above 1 kbar (marked with an asterisk in Figure 4). The majority of the lost signals remain invisible at high pressures, suggesting slow conformational transitions in approximately the millisecond range for the part in the proximity of the C-terminus. We note that the cross-peak intensities for residues 55 and 90 lose their intensity at low pressures (Figure 6A). Their signals are severely broadened even at atmospheric pressure, probably due to slow local fluctuations, which is enhanced at high pressures.

Altogether, we conclude that SUMO-2 has local disorders for the entire segment from residue 54 to 56 and that from residue 88 to 90, which increase above 1.0−1.5 kbar. The

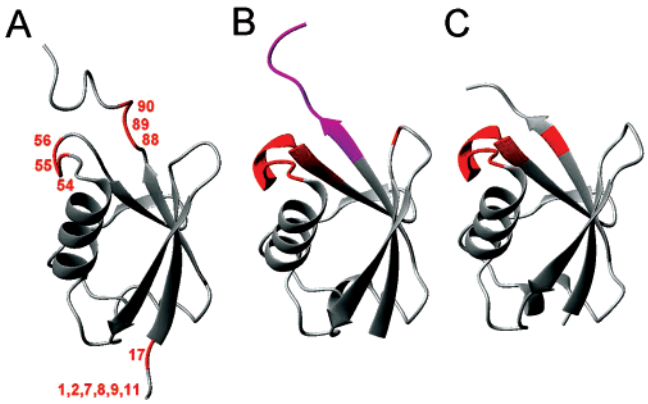

FIGURE 7: Common conformational fluctuations among SUMO-2 (A), ubiquitin (B), and NEDD8 (C). The regions showing characteristic disorder are colored red (residues 1, 2, 7−9, 11, 17, 54−56, and 88−90 for SUMO-2, residues 8, 33, 35, 36, and 39−42 for ubiquitin, and residues 33−42, 68, and 70 for NEDD8). The C-terminal residues (70−76; colored purple) of ubiquitin show clear reorientation with the conformational fluctuation (*15*, *16*).

degree of disorder is slightly different for different residues, creating a locally disordered ensemble of conformers, hereafter designated "conformer I". Conformer I is not newly produced by pressure but simply increases its population at high pressures because of its smaller partial volume in solution relative that of the basic folded conformer (*35*). This will be accompanied by a small degree of "compression" of the protein structure, which generally remains within the intrinsic range of fluctuation. Extrapolation of the Gibbs energy difference to 1 bar through eq 2 gives an estimate of the population of conformer I at 1 bar, which will be discussed in the next section.

The low-populated conformer I of SUMO-2 shows characteristic disorder in residues 54−56 in the loop (residues 53−59) and in residues 88−90 in the C-terminal segment (residues beyond 87), which carries the reactive C-terminal glycine (Figure 7A). Interestingly, the region of disorder in conformer I for SUMO-2 nearly coincides with those in conformer I for ubiquitin (Figure 7B) (*16*) and for NEDD8 (Figure 7C) (*17*). The fact that the same peculiar local disorder is found in the C-terminal proximal parts of the three modifier proteins strongly suggests that the peculiar local disorder is evolutionarily designed for their common function, namely, binding to their target enzymes, E1 and E2. The idea is supported by the fact that the disordered region of conformer I coincides largely with the region of segments that are in direct contact with enzyme E1 or E2 (Figure 7A, for SUMO-2) (*12*, *13*, *17*, *39*, *40*). It seems natural to consider that the disorder in the enzyme-binding segments facilitates binding of the modifier protein to the E1 or E2 enzyme. On the other hand, the sequence variety among the three proteins will determine their specificity of binding for particular E1 and E2 enzymes (*12*).

To examine whether the peculiar local disorder in the rare conformer is common to all UBLs or peculiar to the post-translational modifier, we also carried out a variable-pressure NMR study on a non-post-translational modifier, the N-terminal UBL domain of parkin, which acts as a RING-type E3 ubiquitin ligase (*41*) and shares 32% sequence identity with ubiquitin. We found that, unlike SUMO-2, NEDD8, and ubiquitin, the N-terminal UBL domain of parkin undergoes a simple folding−unfolding transition rather than

Table 2: Comparison of Thermodynamic Parameters for the Transitions from the Basic Folded Conformer (N) to the Alternative Conformer (I) and from the Basic Folded Conformer (N) to the Unfolded Conformer (U) in SUMO-2, Ubiquitin, and NEDD8

	SUMO-2	ubiquitin	NEDD8
temperature (°C)	25	0	30
pH	7.0	4.5	6.0
ΔG^0_{NI} (kJ/mol)	9.1 ± 0.7	15.2 ± 1.0	$<5.3 \pm 2.6$
ΔV^0_{NI} (mL/mol)	-44 ± 3	-58 ± 4	$<-66 \pm 20$
ΔG^0_{NU} (kJ/mol)	22.5 ± 2.0	31.3 ± 4.7	11.0 ± 1.5
ΔV^0_{NU} (mL/mol)	-85 ± 8	-85 ± 7	-70 ± 9

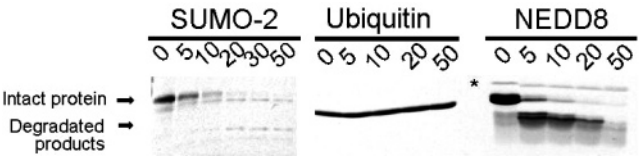

FIGURE 8: Enzymatic degradation assays with chymotrypsin (3 μM) on SUMO-2 (30 μM), ubiquitin (31 μM), and NEDD8 (74 μM) at pH 7.0 and 37 °C at different incubation times from 0 to 50 min, displayed on a SDS−PAGE gel. An impurity band is shown by the asterisk. Experimental procedures for the assays are described in detail in the literature (*17*).

the three-state transition involving an intermediate conformer (data not shown). This observation supports the view that the local disorder in conformer I in the proximity of the C-terminal segment is peculiar for modifier proteins, but not for all UBLs (*17*).

Thermodynamic Design of Post-Transcriptional Ubiquitin-like Modifier Proteins. The foregoing result indicates that conformer I is in equilibrium with the folded (native) conformer (N), namely, N ⇌ I. Furthermore, above 2 kbar, the magnitudes of all the cross-peaks decreased in a concerted manner (Figure 6A), showing the onset of unfolding of the entire polypeptide chain, producing the totally unfolded conformer U. All the conformational changes are reversible with pressure, allowing thermodynamic analysis of the experimental data according to eqs 1 and 2 based on the assumption for the minimum conformational equilibrium for SUMO-2, N ⇌ I ⇌ U.

The red and black circles in Figure 6B depict average degrees of transition for N to I and N to U, respectively. Using eq 2 and extrapolating ΔG to 1 bar, we obtain a ΔG^0_{NI} of 9.1 ± 0.7 kJ/mol for the transition from N to I and a ΔG^0_{NU} of 22.5 ± 2.0 kJ/mol for the transition from N to U, both at 25 °C. The equilibrium population of I at 1 bar is ~2.5% and that of U ~0.01%. They are indeed rare conformers, hard to detect at ambient pressure, but easily detected at high pressures because their populations increase enormously due to their smaller partial volumes relative to that of N (eq 2). The slope of ΔG against pressure gives estimates of partial molar volume changes: $\Delta V^0_{NI} = -44 \pm 3$ mL/mol for the transition from N to I and $\Delta V^0_{NU} = -85 \pm 8$ mL/mol for the transition from N to U (at 1 bar and 25 °C). The volume decreases as the polypeptide chain is progressively more hydrated and disordered. Table 2 compares the thermodynamic parameters determined for SUMO-2 with those previously determined for ubiquitin and NEDD8 under slightly different conditions. The ΔV^0 values for the N to I transition are substantial and are mutually comparable (−44 mL/mol to greater than −66 mL/mol) in the three proteins. The decrease in partial molar volume in a related high-energy conformer of ubiquitin (N′, $\Delta V = -24$ mL/mol) (*14*, *15*) is shown by statistical calculation to be due to the penetration of water molecules into a specific part of the protein (*42*). The substantial and nearly common loss of volume by the N to I transition in the three proteins suggests that the hydration states of the I conformers are fairly similar among the three proteins, as expected from their structural similarity.

Despite the fair degree of similarity in structure and hydration, the thermodynamic stabilities of N and I are far smaller for SUMO-2 and NEDD8 than for ubiquitin. One should note that, although the stabilities of N and I are compared at different pHs and temperatures for the three proteins, the difference would increase if the experiments were conducted under exactly the same condition. This is because the conformational stability of ubiquitin would become even higher if the experiment were conducted for ubiquitin at pH >4.5 and at >0 °C (*43*, *44*).

In the previous work (*17*), we showed that the degradation of NEDD8 by a protease (e.g., chymotrypsin) occurs much more readily than that of ubiquitin. The acceleration of enzymatic degradation for NEDD8 was explained by the substantially higher equilibrium concentration of the unfolded conformer in NEDD8. Here, we compared the enzymatic degradation of SUMO-2 with those of ubiquitin and NEDD8. Although the reactions are compared under slightly different conditions for different proteins, it is clear that SUMO-2 is much more easily degraded than ubiquitin (Figure 8). In living cells, this would make SUMO-2 much more short-lived than ubiquitin. On the other hand, one can easily speculate that, with a higher equilibrium population of the "specifically disordered" conformer I, SUMO-2 and NEDD8 may have much higher reactivities with its target enzyme than ubiquitin. These differences in thermodynamic design among the post-transcriptional UBL modifier proteins may play key roles in their specific function by controlling their level of reactivity and their lifetimes for performing their specific needs in cell physiology.

CONCLUSION

We have demonstrated that the basic folded conformer (N) of human SUMO-2, a UBL post-transcriptional modifier, assumes a $\beta\beta\alpha\beta\beta\alpha\beta$ ubiquitin fold with its main chain conformation being almost identical with those of other post-transcriptional modifiers, ubiquitin and NEDD8. We have further demonstrated that, under physiological conditions, SUMO-2 undergoes conformational fluctuations producing an ensemble of low-populated alternate conformers (I) with peculiar local disorder in the segments in the proximity of the C-terminus, which bind enzyme E1 or E2. Interestingly, similar alternative conformers, with local disorder in the enzyme-binding segments in the proximity of the C-terminus, are found in ubiquitin and NEDD8. Accordingly, we suggest that the peculiar local disorder in the alternative conformers is a strategic design for post-transcriptional UBL modifiers to facilitate their binding to target enzymes. In contrast to the similarity in structure, the thermodynamic stability of I and U with respect N is radically different among the three proteins, giving enormously different equilibrium populations of I and U under physiological conditions. This thermodynamic property difference leads to different levels of de-

gradability of these proteins by protease. There is speculation that differences in thermodynamic stability may critically determine levels of activity of post-transcriptional UBL modifier proteins in living cells despite their outstanding similarity in the basic folded structure and even in the locally disordered conformer.

Finally, the work presented here has clearly demonstrated that a group of proteins with quite similar folds, e.g., UBLs, in the lowest-energy states can behave quite differently in their fluctuations over their energy landscape. Details of such fluctuations, including intermediate structures and their thermodynamics, can be studied in depth by NMR spectroscopy at varying pressures.

ACKNOWLEDGMENT

We thank Sumio Sugano, Akiko Tanaka, Takashi Yabuki, Masaaki Aoki, Eiko Seki, Takayoshi Matsuda, Emi Nunokawa, Mikako Shirouzu, Naomi Ohbayashi, and Takaho Terada for their contributions in protein preparation.

REFERENCES

1. Johnson, R. R., and Hochstrasser, M. (1997) SUMO-1: Ubiquitin gains weight, *Trends Cell Biol. 7*, 408−413.
2. Kiel, C., and Serrano, L. (2006) The ubiquitin domain superfold: Structure-based sequence alignments and characterization of binding epitopes, *J. Mol. Biol 355*, 821−844.
3. Hochstrasser, M. (2000) Evolution and function of ubiquitin-like protein-conugation systems, *Nat. Cell Biol. 2*, E153−E157.
4. Tateishi, K., Omata, M., Tanaka, K., and Chiba, T. (2001) The NEDD8 system is essential for cell cycle progression and morphogenetic pathway in mice, *J. Biol. Chem. 155*, 571−579.
5. Melchior, F. (2000) SUMO-Nonclassical ubiquitin, *Annu. Rev. Cell Dev. Biol. 16*, 591−626.
6. Hay, R. T. (2001) Protein modification by SUMO, *Trends Biochem. Sci. 26*, 332−333.
7. Muller, S., Hoege, C., Pyrowolakis, G., and Jentch, S. (2001) SUMO, ubiquitin's mysterious cousin, *Nat. Rev. 2*, 202−210.
8. Watts, F. Z. (2004) SUMO modification of proteins other than transcription factors, *Cell Dev. Biol. 15*, 211−220.
9. Gutierrez, G. J., and Ronai, Z. (2006) Ubiquitin and SUMO systems in the reguration of mitotic checkpoints, *Trends Biochem. Sci. 31*, 324−332.
10. Bohren, K. M., Nadkarni, V., Song, J. H., Gabbay, K. H., and Owerbach, D. (2004) A M55V polymorphism in a novel SUMO gene (SUMO-4) differentially activates heat shock transcription factors and is associated with susceptability to type I diabetes mellitus, *J. Biol. Chem. 279*, 27233−27238.
11. Bayer, P., Arndt, A., Metzger, S., Mahajan, R., Melchior, F., Jaenicke, R., and Becker, J. (1998) Structure determination of the small ubiquitin-related modifier SUMO-1, *J. Mol. Biol. 280*, 275−286.
12. Ding, H., Xu, Y., Chen, Q., Dai, H., Tang, Y., Wu, J., and Shi, Y. (2005) Solution structure of human SUMO-3 C47S and its binding surface for UBC9, *Biochemistry 44*, 2790−2799.
13. Huang, W. C., Ko, T. P., Li, S. S. L., and Wang, A. H.-J. (2004) Crystal structures of the human SUMO-2 protein at 1.6 Å and 1.2 Å resolution: Implication on the functional differences of SUMO proteins, *Eur. J. Biochem. 271*, 4114−4122.
14. Kitahara, R., Yamada, H., and Akasaka, K. (2001) Two folded conformers of ubiquitin revealed by high-pressure NMR, *Biochemistry 40*, 13556−13563.
15. Kitahara, R., and Akasaka, K. (2003) Close identity of a pressure-stabilized intermediate with a kinetic intermediate in protein folding, *Proc. Natl. Acad. Sci. U.S.A. 100*, 3167−3172.
16. Kitahara, R., Yokoyama, S., and Akasaka, K. (2005) NMR snapshots of a fluctuating protein structure: Ubiquitin at 30 bar-3 kbar, *J. Mol. Biol. 347*, 277−285.
17. Kitahara, R., Yamaguchi, Y., Sakata, E., Kasuya, T., Tanaka, K., Kato, K., Yokoyama, S., and Akasaka, K. (2006) Evolutionally conserved intermediates between ubiquitin and NEDD8, *J. Mol. Biol. 363*, 395−404.
18. Kigawa, T., Yabuki, T., Yoshida, Y., Tsutsui, M., Ito, Y., Shibata, T., and Yokoyama, S. (1999) Cell-free production and stable-isotope labeling of milligram quantities of proteins, *FEBS Lett. 442*, 15−19.
19. Kigawa, T., Yabuki, T., Matsuda, N., Matsuda, T., Nakajima, R., Tanaka, A., and Yokoyama, S. (2004) Preparation of *Escherichia coli* cell extract for highly productive cell-free protein expression, *J. Struct. Funct. Genomics 5*, 63−68.
20. Matsuda, T., Koshiba, S., Tochio, N., Seki, E., Iwasaki, N., Yabuki, T., Inoue, M., Yokoyama, S., and Kigawa, T. (2007) Improving cell-free protein synthesis for stable-isotope labeling, *J. Biomol. NMR 37*, 225−229.
21. Wuthrich, K. (1986) *NMR of Proteins and Nucleic Acids*, John Wiley & Sons, Inc., New York.
22. Ikura, M., Kay, L. E., and Bax, A. (1990) A novel approach for sequential assignment of ^{1}H, ^{13}C, and ^{15}N spectra of proteins: Heteronuclear triple-resonance three-dimensional NMR spectroscopy. Application to calmodulin, *Biochemistry 29*, 4659−4667.
23. Bax, A. (1994) Multidimensional nuclear magnetic resonance methods for protein studies, *Curr. Opin. Struct. Biol. 4*, 738−744.
24. Cavanagh, J., Fairbrother, W. J., Palmer, A. G., and Skelton, N. J. (1996) *Protein NMR Spectroscopy, Principles and Practice*, Academic Press, New York.
25. Delaglio, F., Grzesiek, S., Vuister, G. W., Zhu, G., Pfeifer, J., and Bax, A. (1995) NMRPipe: A multidimensional spectral processing system based on UNIX pipes, *J. Biomol. NMR 6*, 277−293.
26. Johnson, B. A., and Blevins, R. A. (1994) NMRView: A computer program for the visualization and analysis of NMR data, *J. Biomol. NMR 4*, 603−614.
27. Kobayashi, N., Iwahara, J., Koshiba, S., Tomizawa, T., Tochio, N., Guntert, P., Kigawa, T., and Yokoyama, S. (2007) KUJIRA, a package of integrated modules for systematic and interactive analysis of NMR data directed to high-throughput NMR structure studies, *J. Biomol. NMR 39*, 31−52.
28. Schubert, M., Labudde, D., Oschkinat, H., and Schmieder, P. (2002) A software tool for the prediction of Xaa-Pro peptide bond conformations in proteins based on ^{13}C chemical shift statistics, *J. Biomol. NMR 24*, 149−154.
29. Cornilescu, G., Delaglio, F., and Bax, A. (1999) Protein backbone angle restraints from searching a database for chemical shift and sequence homology, *J. Biomol. NMR 13*, 289−302.
30. Güntert, P., Mumenthaler, C., and Wüthrich, K. (1997) Torsion angle dynamics for NMR structure calculation with the new program DYANA, *J. Mol. Biol. 273*, 283−298.
31. Laskowski, R. A., Rullmann, J. A., MacArthur, M. W., Kaptain, R., and Thornton, J. M. (1996) AQUA and PROCHECK-NMR: Programs for checking the quality of protein structures solved by NMR, *J. Biomol. NMR 8*, 477−486.
32. Koradi, R., Billeter, M., and Wüthrich, K. (1996) MOLMOL: A program for display and analysis of macromolecular structures, *J. Mol. Graphics 14*, 51−55.
33. Herrmann, T., Güntert, P., and Wüthrich, K. (2002) Protein NMR structure determination with automated NOE assignment using the new software CANDID and the torsion angle dynamics algorithm DYANA, *J. Mol. Biol. 319*, 209−227.
34. Akasaka, K., and Yamada, H. (2001) On-Line Cell High Pressure Nuclear Magnetic Resonance Technique: Application to Protein Studies, in *Methods in Enzymology, Volume 338: Nuclear Magnetic Resonance of Biological Macromolecules, Part A* (James, T. L., et al., Eds.) pp 134−158, Academic Press, New York.
35. Akasaka, K. (2006) Probing conformational fluctuation of proteins by pressure perturbation, *Chem. Rev. 106*, 1814−1835.
36. Yamada, H., Nishikawa, K., Honda, M., Shimura, T., Tabayashi, K., and Akasaka, K. (2001) Pressure-resisting cell for high-pressure, high-resolution nuclear magnetic resonance measurements at very high magnetic fields, *Rev. Sci. Instrum. 72*, 1463−1471.
37. Kumar, A., Srivastava, S., and Hosur, R. V. (2007) NMR characterization of the energy landscape of SUMO-1 in the native-state ensemble, *J. Mol. Biol. 367*, 1480−1493.
38. Mishra, R. K., Jatian, S. S., Kumar, A., Simhadri, V. R., Hosur, R. V., and Mittal, R. (2004) Dynamin interacts with members of the sumoylation machinery, *J. Biol. Chem. 279*, 31445−31454.
39. Walden, H., Podgorski, M. S., Huang, D. T., Miller, D. W., Howard, R. J., Minor, D. L., Jr., Holton, J. M., and Shulman, B. A. (2003) The structure of the APPBP1-UBA3-NEDD8-ATP

complex reveals the basis for selective ubiquitin-like protein activation by an E1, *Mol. Cell 12*, 1427−1437.

40. Miura, T., Klaus, W., Gsell, B., Miyamoto, C., and Senn, H. (1999) Characterization of the binding interface between ubiquitin and class I human ubiquitin-conjugating enzyme 2b by multidimensional heteronuclear NMR spectroscopy in solution, *J. Mol. Biol. 290*, 213−228.
41. Sakata, E., Yamaguchi, Y., Kurimoto, E., Kikuchi, J., Yokoyama, S., Yamada, S., Kawahara, H., Yokosawa, H., Hatori, N., Mizuno, Y., Tanaka, K., and Kato, K. (2003) Parkin binds the Rpn10 subunit of 26S proteasomes through its ubiquitin-like domain, *EMBO Rep. 4*, 301−306.
42. Imai, T., Ohyama, S., Kovalenko, A., and Hirata, F. (2007) Theoretical study of the partial molar volume change associated with the pressure-induced structural transition of ubiquitin, *Protein Sci. 16*, 1927−1933.
43. Ibara-Molero, B., Loladze, V. V., Makhatadze, G. I., and Sanchez-Ruiz, J. M. (1999) Thermal versus guanidine-induced unfolding of ubiquitin. An analysis in terms of the contributions from charge-charge interactions to protein stability, *Biochemistry 38*, 8138−8149.
44. Ibarra-Molero, B., Makhatadze, G. I., and Sanchez-Ruiz, J. M. (1999) Cold denaturation of ubiquitin, *Biochim. Biophys. Acta 1429*, 384−390.

BI7014458